Proc. Natl. Acad. Sci. USA
Vol. 95, pp. 6492–6497, May 1998
Neurobiology

Heterogeneity of subcellular localization and electrophoretic mobility of survival motor neuron (SMN) protein in mammalian neural cells and tissues

JONATHAN W. FRANCIS*, ALFRED W. SANDROCK*, PRADEEP G. BHIDE*, JEAN-PAUL VONSATTEL*†, AND ROBERT H. BROWN, JR.*‡

Departments of *Neurology and †Pathology, Massachusetts General Hospital and Harvard Medical School, Building 149, 13th Street, Charlestown, MA 02129

Communicated by Louis M. Kunkel, Harvard Medical School, Boston, MA, March 23, 1998 (received for review August 18, 1997)

ABSTRACT **Spinal muscular atrophy is caused by defects in the survival motor neuron (SMN) gene. To better understand the patterns of expression of SMN in neuronal cells and tissues, we raised a polyclonal antibody (abSMN) against a synthetic oligopeptide from SMN exon 2. AbSMN immunostaining in neuroblastoma cells and mouse and human central nervous system (CNS) showed intense labeling of nuclear "gems," along with prominent nucleolar immunoreactivity in mouse and human CNS tissues. Strong cytoplasmic labeling was observed in the perikarya and proximal dendrites of human spinal motor neurons but not in their axons. Immunoblot analysis revealed a 34-kDa species in the insoluble protein fractions from human SY5Y neuroblastoma cells, embryonic mouse spinal cord cultures, and human CNS tissue. By contrast, a 38-kDa species was detected in the cytosolic fraction of SY5Y cells. We conclude that SMN protein is expressed prominently in both the cytoplasm and nucleus in multiple types of neurons in brain and spinal cord, a finding consistent with a role for SMN as a determinant of neuronal viability.**

Spinal muscular atrophy (SMA) is an autosomal recessive neuromuscular disease characterized by early degeneration of α-motor neurons in the ventral horn of the spinal cord. The most severe form, variably termed SMA type I, acute SMA, or Werdnig-Hoffman disease, is the most common genetic cause of infant mortality (1). The genetic abnormality for SMA type I and its milder variants (SMA types II, III, and IV) has been mapped by linkage analysis to chromosome 5q13 (2–4).

The primary cause of SMA derives from mutations in a novel survival motor neuron (SMN) gene located in the SMA locus (5, 6). The SMN gene is present in almost identical centromeric (*SMN*^{C}) and telomeric (*SMN*^{T}) copies. Exon 7 from *SMN*^{T} is homozygously deleted in approximately 95% of SMA patients (5, 7–10). Perhaps more importantly, there are a growing number of intragenic mutations in *SMN*^{T} that have been identified in SMA patients who possess at least one nondeleted *SMN*^{T} allele (5, 7, 8, 11–13). These intragenic mutations are less frequent than gross deletions, but the fact that they cause the SMA phenotype argues strongly for the specificity of *SMN*^{T} as the critical gene in SMA. It most recently has been shown that there is a marked deficiency of the SMN protein in SMA patients as well (14, 15).

The cDNA of the *SMN*^{T} gene encodes a putative protein of 294 amino acids (estimated M_r = 32,000) that interacts both with other proteins and with RNAs (5, 16–18). A yeast two-hybrid screen for protein–protein interactions first demonstrated that the SMN protein interacts with (*i*) the small nucleolar RNA binding protein, fibrillarin, and (*ii*) a RNA binding domain present in the carboxyl terminal region of the heterogeneous nuclear mRNA binding protein, hnRNP U (16). In that study, immunostaining of cultured cell lines with a monoclonal anti-SMN antibody (abSMN) revealed intense labeling of several intranuclear dots termed "gems." Gems were found to be similar in number and size to nuclear coiled bodies and frequently were seen in close association with coiled bodies as shown by double-label immunofluorescence experiments with either anti-p80-coilin or antifibrillarin antibodies. The SMN protein since has been shown to bind directly to certain small nuclear RNAs and a number of other proteins that participate together in early spliceosome assembly within the cytoplasm of *Xenopus* oocytes (17, 18). Although these studies suggest that SMA may result from a defect in cellular posttranscriptional RNA metabolism secondary to a deficiency of SMN protein, it is still unclear how SMN protein loss contributes to the selective loss of ventral horn motor neurons that characterizes SMA.

Inasmuch as all of the studies looking at cellular function of SMN have been done in non-neural cells, little is known about the distribution and function of the SMN protein in the neural cells and tissues known to be affected by SMA pathology. The few reported studies of SMN protein expression in mammalian central nervous system (CNS) tissues have so far yielded mostly general findings (14, 15, 19). Western blot analysis has shown that the SMN protein is abundantly expressed in human brain and spinal cord although it is detected at similar levels in non-neural tissues as well (15). Consistent with this, immunostaining experiments have demonstrated strong SMN labeling within the cytoplasm of certain groups of neurons distributed throughout the mammalian CNS, including spinal motor neurons (14, 19). However, observation of gems in the mammalian CNS so far has been limited to fetal human spinal cord motor neurons (14). To extend our understanding of SMN protein expression in brain and spinal cord, we have characterized the subcellular localization and electrophoretic behavior of SMN in cultured neural cells and mouse and human CNS tissues.

MATERIALS AND METHODS

AbSMN Preparation. A polyclonal antibody to a synthetic oligopeptide derived from the predicted human SMN amino acid sequence for exon 2 (amino acids 60–76) was raised in rabbits after conjugation of the peptide to keyhole limpet hemocyanin (KLH). The amino terminus of this peptide is a native cysteine residue that was used for conjugation of the peptide to KLH and to a thiol-reactive chromatography sup-

The publication costs of this article were defrayed in part by page charge payment. This article must therefore be hereby marked "*advertisement*" in accordance with 18 U.S.C. §1734 solely to indicate this fact.

Abbreviations: SMA, spinal muscular atrophy; SMN, survival motor neuron; abSMN, anti-SMN antibody; CNS, central nervous system.

‡To whom reprint requests should be addressed at: Cecil B. Day Laboratory for Neuromuscular Research, Massachusetts General Hospital, East, Building 149, 13th Street, Room 6627, Charlestown, MA 02129. e-mail: brown@helix.mgh.harvard.edu.

port for affinity purification of abSMN (Pierce). To assess antibody specificity, two recombinant SMN fusion proteins were expressed in bacteria for use as positive controls in immunoblot studies. Both contained the full-length coding region of wild-type human SMN cDNA joined to either the C-terminal 460 amino acids of tetanus toxin (fusion protein 1) (20) or a modified form of *Escherichia coli* thioredoxin (fusion protein 2; Invitrogen). A second polyclonal antibody, chicken anti-human SMN antisera C3 was obtained from Dan Coovert and Arthur Burghes at Ohio State University (15).

Immunocytochemical and Western Blot Studies of SY5Y Cells. Human SH-SY5Y neuroblastoma cells were cultured in DMEM (GIBCO/BRL) containing 10% fetal calf serum, 100 units/ml of penicillin/streptomycin, and 2.5 μg/ml of amphotericin B (21). For immunolabeling studies, paraformaldehyde-fixed cells were permeabilized-blocked in PBS containing 2% normal goat serum/0.1% Triton X-100 and then incubated with primary antibodies for 2 hr at room temperature (abSMN, 200 ng/ml; monoclonal mouse anti-coilin hybridoma culture supernatant, 1:150). Cultures subsequently were incubated with fluorochrome-labeled secondary antibodies (Jackson ImmunoResearch; Cy3 Goat anti-rabbit IgG, 1:1,000; fluorescein isothiocyanate goat anti-mouse IgG, 1:250) for 30 min.

For immunoblot studies, 1–2 $\times$ 10^7 cells were subjected to subcellular fractionation according to previously described methods (22). Briefly, dissociated cells were pelleted in a 1.5-ml microcentrifuge tube and resuspended in 0.5 ml of ice-cold buffer A [10 mM Hepes, pH 7.9, containing 10 mM KCl, 0.1 mM EDTA, 0.1 mM EGTA, 1 mM DTT, 0.5 mM phenylmethylsulfonyl fluoride (PMSF), 2 μg/ml of leupeptin, and 2 μg/ml of pepstatin]. The cell suspension was incubated on ice for 15 min, after which 25 μl of a 10% solution of Nonidet P-40 was added. After vigorous vortexing for 10 sec, the nuclei were pelleted by centrifugation at 800 *g* for 3 min. The translucent nuclear pellet was resuspended by trituration in 100 μl of buffer C (20 mM Hepes, pH 7.9, containing 0.4 M NaCl, 1 mM EDTA, 1 mM EGTA, 1 mM DTT, 1 mM PMSF, 2 μg/ml of leupeptin, and 2 μg/ml of pepstatin) and incubated on ice for 15 min with intermittent resuspension. The mixture then was centrifuged at 15,000 *g* for 10 min at 4°C. The resulting supernatant (soluble nuclear extract) was removed with a pipette and the insoluble nuclear pellet was dispersed by sonication in 100 mM Tris·HCl, pH 7.4, containing 1% SDS, 5 mM EDTA, 1 mM DTT, 1 mM PMSF, 2 μg/ml of leupeptin, and 2 μg/ml of pepstatin. Proteins were resolved by SDS/PAGE on a 4–15% gradient gel (Bio-Rad) and transferred to nitrocellulose (23). After a 30-min incubation in primary antibody (abSMN, 125 ng/ml), immunoreactive bands were detected by using avidin-biotin immunochemistry with alkaline phosphatase as the reporter enzyme (Vector Laboratories). Antibody preadsorption controls were carried out by overnight incubation of 2.5 μg/ml of abSMN with either the exon 2 or an exon 4 peptide at a concentration of 40 μg/ml. These preadsorbed antibody solutions then were diluted to a final antibody concentration of 125 ng/ml immediately before incubation with the immunoblot. Immunoblots carried out with chicken anti-SMN antisera C3 were performed by using enhanced chemiluminescence detection as previously described (15).

Immunocytochemical and Western Blot Studies of Mouse Embryo Spinal Cord Cultures. Spinal cord cultures were prepared from embryonic NDH Swiss–Webster mice (Harland Laboratories, Haslett, MI) at 13 days gestation. Cells were plated at a density of 5 $\times$ 10^5 cells per 1 cm^2 well on laminin-treated glass microscope slides and were cultured in MEM (GIBCO/BRL) supplemented with 100 units/ml of penicillin, 50 μg/ml of streptomycin, 2 mM glutamine, 1 mM pyruvate, 10% fetal calf serum, and 2% chicken embryo extract. Astrocyte-enriched glial cultures were prepared by using forebrain tissues from p0 Sprague–Dawley rats (24). After 5 days *in vitro*, spinal cord cultures were processed for double-label immunofluorescence as described above (abSMN, 200 ng/ml; mouse mAb against Islet-1, 1:50). Soluble and insoluble protein fractions from the spinal cord and mixed cortical glial cultures were studied by Western blot analysis.

Immunohistochemical and Western Blot Studies of Human CNS. Frozen adult human CNS tissue was obtained from normal autopsy material as determined by standard neuropathological review (Alzheimer's Disease Research Center, Massachusetts General Hospital). For immunohistochemical experiments, frozen sections (10 μm) were fixed in acetone for 5 min and washed in PBS. After a 30-min incubation in blocking/permeabilization buffer containing 0.03% H_2O_2, sections were incubated overnight in abSMN at a concentration of 200 ng/ml. Subsequent incubations with biotinylated secondary antibodies (1:600) and avidin-biotin peroxidase complex were performed according to the manufacturer's instructions (Vector Laboratories). Antibody preadsorption controls were carried out by overnight preincubation of abSMN with its peptide antigen at concentrations of 10 μg/ml and 86 μg/ml, respectively. For Western blot analysis, frozen cerebellum was homogenized in 100 mM PBS, pH 7.4, containing 0.5% Nonidet P-40, 1 mM DTT, 5 mM EDTA, and antiproteases. This total homogenate was centrifuged at 800 *g* for 10 min to yield a low-speed supernatant (S1) and pellet (P1). The pellet subsequently was solubilized by sonication in 100 mM Tris·HCl, pH 7.4, containing 1% SDS, 1 mM DTT, 5 mM EDTA, and antiproteases. Tissue extracts (20 μg total protein) were subject to immunoblot analysis with abSMN and C3 antisera as described above.

Immunohistochemical and Western Blot Studies of Adult Mouse CNS. Female adult CD-1 mice (20 weeks of age, 40 g) were anesthetized with a ketamine/xylezine mixture and perfused with 4% paraformaldehyde in 0.1 M phosphate buffer, pH 7.3. Frozen sections (10 μm) were prepared from postfixed spinal cord that had been cryopreserved overnight in 30% sucrose before cryostat sectioning. In a separate case, a Vibratome was used to cut free-floating sections (50 μm) of both brain and spinal cord after fixation. For both preparations, sections were preincubated for 30 min in blocking/permeabilization buffer containing the additional additives of 1% BSA and 0.03% hydrogen peroxide followed by incubation overnight at 4°C in 100 ng/ml abSMN diluted in blocking buffer. Subsequent incubations with biotinylated secondary antibody and avidin-biotin peroxidase complex were performed according to the manufacturer's instructions (Vector Laboratories). Immunoblot analysis of mouse cerebellar P1 fraction was carried out with abSMN and chicken anti-SMN antisera C3 as described above.

RESULTS

Characterization of Anti-SMN Peptide Antibodies. To demonstrate the antigenic specificity of affinity-purified abSMN, we first verified by immunoblot analysis that the antibody selectively recognized two recombinant SMN fusion proteins present in total soluble protein fractions obtained from the respective bacterial lysates. In each of these bacterial extracts, abSMN reacted with a single predominant protein species at the electrophoretic mobility expected for the expressed fusion construct (Fig. 1*A*). Accordingly, the antibody recognized both an 83-kDa band corresponding to the tetanus toxin-SMN fusion polypeptide of 754 amino acids (fusion protein 1), as well as a 47-kDa band representing the thioredoxin-SMN fusion protein of 430 residues (fusion protein 2).

Immunocytochemical and Western Blot Studies of SY5Y Cells. We also confirmed that our rabbit polyclonal antibody produced the same cellular localization profile of anti-SMN immunoreactivity in human SY5Y neuroblastoma cells as observed previously with mouse mAb 2B-1 (16). AbSMN

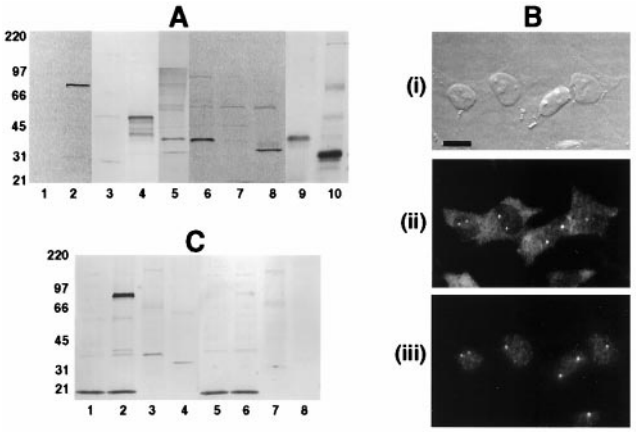

FIG. 1. Characterization of abSMN. (*A*) Immunoblots of *E. coli* expressed SMN fusion proteins and subcellular fractions of human neuroblastoma cells probed with abSMN (lanes 1–8) or chicken anti-human SMN antibody C3 (lanes 9–10). AbSMN reacts with two different fusion constructs expressing wild-type SMN (fusion proteins 1 and 2) but not with extracts from bacteria lacking the SMN cDNA insert or extracts from cells obtained before induction of protein expression. Subcellular fractions of SY5Y cells were probed by using the same abSMN antibody concentration. Lane 1: BL21DE3 bacteria, negative control (2 μg). Lane 2: BL21DE3 bacteria expressing fusion protein 1 (2 μg). Lane 3: DH5α bacteria, negative control (5 μg). Lane 4: DH5α bacteria expressing fusion protein 2 (5 μg). Lane 5: SY5Y cells, total cell lysate (20 μg). Lane 6: SY5Y cells, cytosolic fraction (20 μg). Lane 7: SY5Y cells, soluble nuclear extract (20 μg). Lane 8: SY5Y cells, insoluble nuclear material (20 μg). Lane 9: SY5Y cells, cytosolic fraction (20 μg). Lane 10: SY5Y cells, insoluble nuclear material (20 μg). (*B*) Immunocytochemical localization of SMN in human SY5Y neuroblastoma cells determined by using double-label indirect immunofluorescence. (*i*) Fixed cells viewed when using Hoffman modulation (Bar = 20 μm). (*ii*) abSMN (200 ng/ml) immunostaining demonstrates moderate cytoplasmic labeling and strong labeling of nuclear gems. (*iii*) Simultaneous immunostaining with monoclonal anti-p80-coilin antibody (1:150) shows that abSMN reactive gems are often closely associated with nuclear coiled bodies. (*C*) Preadsorption studies of abSMN. Detection of SMN protein by immunoblot analysis persists after preincubation of abSMN with an exon 4 oligopeptide (lanes 1–4), whereas preadsorption with the appropriate exon 2 peptide eliminates SMN immunoreactivity (lanes 5–8). Lanes 1 and 5: BL21DE3 bacteria, negative control (2 μg). Lanes 2 and 6: BL21DE3 bacteria, fusion protein 1 (2 μg). Lanes 3 and 7: SY5Y cells, cytosolic fraction (20 μg). Lanes 4 and 8: SY5Y cells, insoluble nuclear material (10 μg).

typically produced strong labeling of two or three discrete round dots, or "gems," located in the cell nucleus, accompanied by a lower level of fine, granular cytoplasmic immunostaining (Fig. 1*B-ii*). Double-label experiments with anti-p80-coilin mAb further verified that the nuclear dots recognized by abSMN were often in close association with coiled bodies (Fig. 1*B-iii*).

Finally, Western blot analysis of subcellular fractions from SY5Y cell lysates verified that our antibody recognizes an endogenous cellular protein having the predicted size for SMN. Total cell lysates revealed a single predominant band corresponding to a M_r of 38,000 (Fig. 1*A*). A second, minor immunoreactive band with a M_r of 34,000 was also occasionally seen in some of our total lysate preparations. However, when SY5Y cells were subject to subcellular fractionation, each of these bands was selectively localized in a different subcellular fraction: the 38-kDa band remained in the soluble, cytosolic fraction whereas the 34-kDa immunoreactive band had become the major band in the insoluble nuclear material. Review of the protein concentrations for these samples indicated that the fractionation protocol produced a 7-fold enrichment of the 34-kDa band in the insoluble nuclear fraction relative to the total cell lysate. This subcellular fractionation pattern of SMN immunoreactivity was confirmed in a subsequent immunoblot study that used a previously characterized chicken anti-human SMN antisera C3 (15) (Fig. 1*A*). The signal from both of these immunopositive protein species was abolished by preincubation of abSMN with its corresponding exon 2 peptide (Fig. 1*C*), but not with a synthetic oligopeptide derived from SMN exon 4. The soluble nuclear extract failed to produce any immunoreaction product within the expected range of mobility. In aggregate, these studies strongly indicate that abSMN possesses the antigen affinity and specificity required for analysis of endogenous SMN protein expression in eukaryotic cells.

Immunocytochemical and Western Blot Studies of Mouse Embryo Spinal Cord Cultures. We next studied the localization of SMN in mixed cultures of dissociated embryonic mouse spinal cord cells. By analogy to the pattern of immunoreactivity in the SY5Y cell line, our mouse spinal cord neurons exhibited strong immunostaining of 2–6 small dots per cell body (Fig. 2*B*). These immunolabeled dots appeared to be somewhat selectively localized in motor neurons as indicated by costaining of abSMN positive cells with anti-Islet-1 antibody (Fig. 2*C*), a marker for immature spinal motor neurons during their early differentiation (25). We did not observe any abSMN immunostaining in the underlying glial monolayer of these cultures. Corresponding Western blot analysis of Nonidet P-40-soluble supernatants and SDS-solubilized pellets prepared from lysates of these spinal cord cultures demonstrated a major immunoreactive band in the insoluble material having an approximate M_r of 34,000 (Fig. 2*D*). Consistent with the lack of anti-SMN immunostaining in cultured spinal cord glial cells, we were unable to detect this band in the insoluble fraction obtained from prepassaged cultures of rat cerebral glial cells. The higher M_r reactive bands observed in the soluble fractions from the neuronal cultures are likely to represent endogenous, biotin-containing carboxylases (26) (J.W.F., unpublished observations). These experiments with primary cultures of mouse spinal cord cells demonstrate that SMN protein is expressed in the particular subset of mammalian CNS neurons that are characteristically afflicted in SMA.

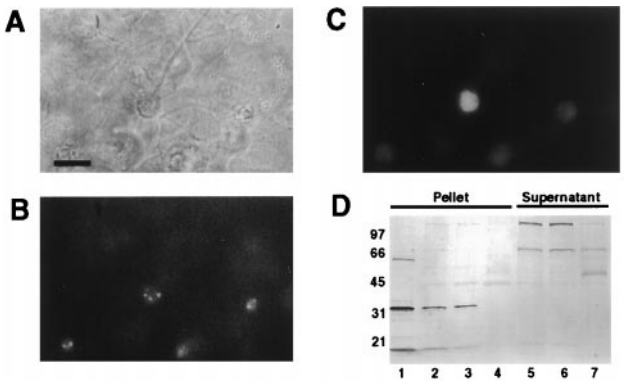

FIG. 2. Immunocytochemical and Western blot analysis of SMN protein in dissociated cultures of mouse embryonic spinal cord. (*A*) Phase contrast micrograph of cultured cells after 7 days *in vitro* (Bar = 30 μm). (*B*) abSMN immunoreactivity is limited to neuronal cell bodies. (*C*) Concurrent labeling of cell shown in *B* with mouse anti-Islet 1 antibody indicates that SMN is present within spinal motor neurons. (*D*) Immunoblot of cell extracts prepared from spinal cord cultures. Samples (8 μg total protein) were probed with 125 ng/ml abSMN. Like SY5Y cells, mixed neuron/glia cultures from spinal cord demonstrated a 34-kDa band in the insoluble protein fraction. Lane 1: SY5Y cell extract, insoluble nuclear fraction. Lane 2: Ventral spinal cord culture, insoluble fraction. Lane 3: Dorsal spinal cord culture, insoluble fraction. Lane 4: Cortical glia culture, insoluble fraction. Lane 5: Ventral spinal cord culture, soluble fraction. Lane 6: Dorsal spinal cord culture, soluble fraction. Lane 7: Cortical glia culture, soluble fraction.

Immunohistochemical and Western Blot Studies of Human CNS Tissues. To define the cellular localization and regional distribution of SMN protein in the human CNS, we performed immunohistochemical analysis of cryosections obtained from selected areas of brain and spinal cord. These studies revealed high levels of abSMN immunoreactivity within the cell bodies and proximal dendrites of large neurons. In particular, cerebral cortical pyramidal cells, cerebellar Purkinje cells, and α-motor neurons in the lumbar spinal cord all showed pronounced staining within their perikarya and proximal dendrites (Fig. 3 *A-E*). abSMN immunolabeling within motor neuron cell bodies frequently was intensely patchy or tigroid, whereas staining within proximal dendrites often appeared as membranous tubes oriented parallel to the longitudinal axis of the dendrite (Fig. 3*D*). In contrast to this strong staining seen in motor neuron cell bodies and dendrites, there was a conspicuous absence of anti-SMN immunoreaction product in spinal motor neuron axons as they passed through the anterior funiculi to exit the cord, and in axons making up the major fiber tracts within the spinal cord white matter (data not shown). Finally, within the areas of brain and spinal cord white matter studied here, we routinely observed scattered, weakly abSMN immunopositive cell nuclei. The number of anti-SMN immunopositive cell nuclei in white matter generally appeared to be only a fraction of the number of cell nuclei identified by routine histological staining of adjacent tissue sections with hematoxylin and eosin (data not shown).

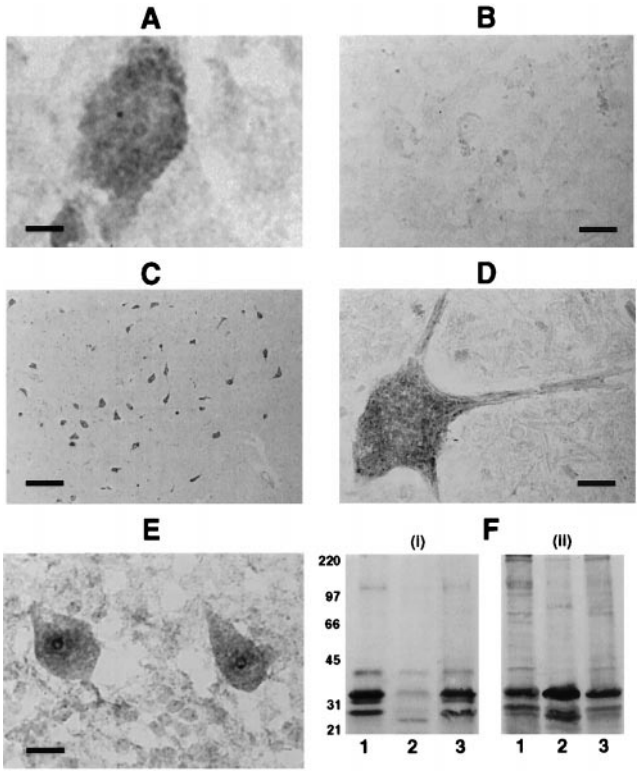

FIG. 3. Immunohistochemical and Western blot analyses of SMN in human CNS tissues. (*A*) Pyramidal neuron in the neocortex shows strong SMN immunolabeling of cytoplasm and nuclear gems. (Bar = 5 μm.) (*B*) Preadsorption of abSMN with 100-fold excess of peptide abolishes staining. (Bar = 50 μm.) (*C*) Low-magnification view of anterior horn cells within ventral gray matter of adult lumbar spinal cord. The cell bodies and proximal dendrites of α-motor neurons are intensely immunoreactive. (Bar = 230 μm.) (*D*) High-power view of adult anterior horn cell. (Bar = 20 μm.) (*E*) SMN labeling of nucleoli in cerebellar Purkinje cells often appeared as a solid ring of immunoreactivity circumscribing the outer surface of the nucleolus. (Bar = 10 μm.) (*F*) Western blot analysis of low-speed pellet material prepared from homogenates of human cerebellar autopsy tissue. After transfer to nitrocellulose, tissue fractions (20 μg total protein) were probed with either abSMN (*i*) or chicken antibody C3 (*ii*). Lanes: 1, autopsy case 96017; 2, autopsy case 97029; 3, autopsy case 97051.

AbSMN immunostaining also demonstrated a single, small, round nuclear dot, or "gem," in many CNS cells located in various regions of gray matter. Gems were more evident in cortical pyramidal cells than in Purkinje cells or α-motor neurons (Fig. 3*A*). The dots did not appear to be immunolabeled cell nucleoli because individual gems were seen along with a separate, larger, weakly stained nucleolus in the same nucleus of a given cortical pyramidal neuron. Although the nucleoli of cortical pyramidal cells typically showed little SMN immunoreactivity, the nucleoli of cerebellar Purkinje cells were more commonly heavily labeled (Fig. 3*E*). The pattern of abSMN nucleolar staining seen in Purkinje cells often revealed a gradient of immunoreactivity such that the outer rim of the nucleolus was much more intensely labeled than the center, with the rim frequently exhibiting one or two caps of immunostained material. Nucleolar staining also has been observed with another polyclonal antibody raised against exon 2 of rat SMN (V. La Bella, personal communication). Preincubation of abSMN with an excess of peptide antigen from exon 2 largely abolished staining in all brain regions studied (Fig. 3*B*, cerebral cortex). Consistent with our immunoblot results using cultured cells, Western blot analysis of human cerebellar tissue extracts also revealed a prominent 34-kDa immunoreactive band present in the low-speed pellet fractions (Fig. 3*F*). This band was present in multiple autopsy specimens and was recognized by both abSMN and chicken anti-SMN antibody C3.

Immunohistochemical and Western Blot Studies of Adult Mouse CNS. To determine whether the profile of abSMN immunoreactivity in human CNS tissue is observed in other mammalian species, we extended our survey of CNS tissues to include mouse brain and spinal cord. Vibratome sections stained with abSMN revealed strong immunoreactivity within neurons located throughout the CNS. This immunostaining was particularly intense within one or two small intranuclear dots, resembling gems as described in multiple other cell types (Fig. 4*A*). In many neurons these appeared as perinucleolar caps that were analogous to the pattern of nucleolar staining seen in human cerebellar Purkinje cells. As in human CNS, abSMN immunolabeling within regions of mouse white matter was weak or absent. Intense SMN immunolabeling of both nucleoli and gems was even more pronounced in anterior horn cells within frozen sections of perfusion-fixed mouse lumbar spinal cord. In this preparation, SMN immunoreactive gems

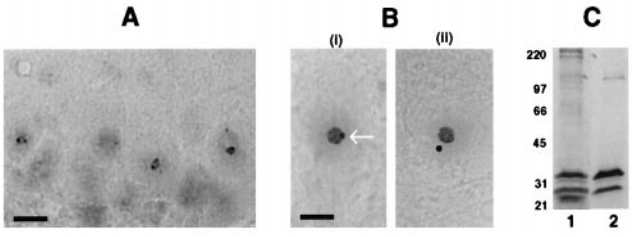

FIG. 4. Immunohistochemical and Western blot analyses of selected CNS tissues from the adult mouse. (*A*) Vibratome section of cerebellum showing Purkinje cells in which abSMN-reactive gems appear to have a perinucleolar localization. No discernible staining of Purkinje cell cytoplasm was observed. (Bar = 8 μm.) (*B*) Frozen sections of lumbar spinal cord reveal strong abSMN immunoreactivity within gems and nucleoli of ventral horn motor neurons. In this preparation, gems were observed in contact with the nucleolus (*i*, arrow) or free in the nucleoplasm (*ii*) (Bar = 3 μm for both *i* and *ii*.) (*C*) Western blot of low-speed pellet material prepared from cerebellum. After transfer to nitrocellulose, tissue samples were probed with either abSMN (lane 1) or chicken antibody C3 (lane 2). In both cases a major 34-kDa band was detected.

were clearly observed as both perinucleolar caps as well as distinct subnuclear structures that were physically separate from the larger, strongly immunopositive nucleolus (Fig. 4*B*). Immunoblot analysis of low-speed pellet fraction from mouse cerebellum revealed a major 34-kDa band that was recognized by both abSMN and chicken anti-SMN antibody C3 (Fig. 4*C*).

DISCUSSION

We have investigated the cellular localization of SMN in various neural cells and mammalian CNS tissues by using a polyclonal antibody raised against a synthetic SMN oligopeptide. As in previous studies that demonstrated widespread expression of SMN throughout a range of human tissues and cell types (5, 14–16), we detected anti-SMN immunoreactive material in SY5Y neuroblastoma cells, embryonic mouse spinal cord cultures, adult mouse CNS, and human CNS autopsy tissue. AbSMN immunostaining identified nuclear "gem-like" structures in most of these preparations whereas Western blot analysis of the corresponding cell lysates or tissue homogenates revealed a 34-kDa immunoreactive species, again in broad agreement with earlier reports (5, 15, 16).

Perhaps the most salient finding in our investigation is the heterogeneous pattern of subcellular immunostaining observed with our antibody in various mammalian CNS tissues. Consistent with previous immunohistochemical analyses of human brain and spinal cord (14, 19), our studies with abSMN showed strong levels of cytoplasmic immunoreactivity within the perikarya and proximal dendrites of large neurons in adult tissue. However, in contrast to earlier results from human, monkey, and rat CNS that reported that neuronal SMN staining is confined to the cytoplasm (19), we observed prominent intranuclear labeling in neurons throughout the mouse CNS and also within certain groups of human CNS neurons. In human cortical pyramidal neurons, abSMN immunostaining identified small, round intranuclear dots that appeared to be gems inasmuch as a single, intensely immunoreactive dot often was seen in the same cell nucleus along with a larger, distinct, albeit weakly stained, nucleolus. abSMN recognized similar "gem-like" dots within the nuclei of other CNS neurons (e.g., cerebellar granule cells), but we are currently hesitant to designate these entities as authentic gems because we were unable to see separate nucleoli within these cells. In comparison to abSMN labeling in human CNS, in which both nuclear and cytoplasmic SMN immunoreactivity were detected, staining in mouse CNS appeared to localize exclusively within the nucleus. The basis for this interspecies difference in immunolabeling pattern is unclear, although it may be related to the fact that there is only one copy of the *SMN* gene in the mouse; unlike the human SMN^{T} and SMN^{C} genes, the mouse *SMN* gene gives rise to only the full-length form of the SMN protein (27).

We have repeatedly seen prominent immunolabeling of neuronal cell nucleoli with abSMN in tissue sections from both mouse and human CNS. This nucleolar staining is consistent with the known binding interaction of SMN with the nucleolar protein, fibrillarin (16), and is also in agreement with the immunolocalization of p80-coilin to perinucleolar caps within neurons from primary cultures of rat hippocampus or cerebellum (28, 29). These findings are corroborated by La Bella and colleagues who observe robust nucleolar immunolabeling in cultured neurons by using a different polyclonal anti-SMN antibody raised against exon 2 of rat SMN (V. La Bella, personal communication). Although this evidence suggests that the SMN protein may have a heretofore undocumented association with nucleoli in certain types of nerve cells, it is unclear why abSMN seemed to selectively stain gems in some types of human neurons (e.g., neocortical pyramidal neurons) and nucleoli in other types (i.e., cerebellar Purkinje cells). Given that the SMN protein is expressed at varying levels in different tissues and cell types (15), the cell-type specific differences in immunocytochemical staining observed here in the human brain and spinal cord ultimately may be a reflection of considerable variations in SMN expression level among subpopulations of CNS neurons.

Our characterization of abSMN immunoreactivity in cultured neural cells produced two other observations: (*i*) In contrast to the single, predominant ≈40-kDa anti-SMN immunoreactive species demonstrated previously in total cell lysates of HeLa cells (16), subcellular fractionation of SY5Y neuroblastoma cells identified two distinct anti-SMN immunoreactive bands having different solubility properties and electrophoretic mobilities: a soluble 38-kDa species present in the cytoplasmic fraction and an insoluble 34-kDa species found in the nuclear fraction. Although the lower M_r band could represent an artifact of proteolysis incurred during sample preparation, our findings also raise the possibility that the SMN protein might be compartmentalized within SY5Y cells as two different isoforms possessing different primary structures and/or different levels of posttranslational modification. Indeed, alternative splicing of both the SMN^{T} and SMN^{C} mRNAs has been identified by analysis of SMN transcripts in lymphoblastoid cell lines and human muscle and CNS tissues (5, 12, 30). Previous studies of the coiled body marker, p80-coilin, indicate that variations in posttranslational modification tied to the cell cycle also could explain the presence of two different SMN protein species in SY5Y cells (28, 31).

(*ii*) Whereas the SMN protein has been identified in a number of non-neuronal cell lines and primary cell types *in vitro* (15, 16), we so far have been unable to detect abSMN immunoreactivity within glial cells present in our primary cultures of embryonic mouse CNS tissues. Accordingly, SMN immunostaining was absent in the underlying glial monolayer of mixed spinal cord cultures, and immunoblot analysis failed to detect an abSMN immunoreactive species within cell lysates of prepassaged glial cultures derived from forebrain tissue. One explanation for this unexpected result may be that growth-arrested cells in culture demonstrate markedly fewer coiled bodies and lower levels of p80-coilin protein as compared with cultures of freely proliferating cells (31). Thus, the lack of abSMN immunoreactivity within cultured glial cells may be attributable to the quiescent state of these cells induced by antimitotic treatment and/or glial cell confluence. Coiled bodies similarly have proved difficult to detect in certain primary cell types such as human fibroblasts (28, 32). Perhaps more importantly, there is considerable evidence suggesting that the constitutive expression level of SMN in CNS glial cells is relatively low. This evidence is based not only on our own observation of sparse abSMN immunoreactivity within white matter regions of mouse and human CNS *in situ*, but also on similar findings from previous immunohistochemical studies of mammalian CNS using other anti-SMN antibodies (14, 19).

Although the physiological significance of SMN immunoreactivity within gems, nucleoli, and the cytoplasm of human CNS neurons has yet to be clearly defined, these findings are broadly consistent with a role for the SMN protein in posttranscriptional RNA processing (16). In support of this, recent studies of *Xenopus* oocyte cytoplasm indicate that SMN may be important in the formation of spliceosomes, in conjunction with certain small nuclear RNAs, SMN-interacting protein 1 (SIP-1), and the core Sm proteins (17, 18). The prominent cytoplasmic immunostaining of SMN within mammalian CNS neurons strongly argues for an analogous function in neuronal cytoplasm and potentially for a role for SMN in chaperoning and trafficking spliceosomes into the nucleus after formation within the cytoplasm. Additionally, the close physical association of SMN-immunoreactive gems with coiled bodies and nucleoli, and the protein-binding interaction of SMN with the coiled body/nucleolar small nucleolar RNA binding protein, fibrillarin (16), constitute formidable evidence linking the

SMN protein to a putative role in the posttranscriptional processing of ribosomal RNA and heteronuclear mRNA within the nucleus. That SMN plays an essential role in some aspect of basic cellular metabolism also is supported by the finding of early embryonic lethality in homozygous SMN knockout mice (27). Further studies of the specificity of binding interactions between SMN and various constituents of the spliceosome and intranuclear transcriptional apparatus may yield valuable information as to the cellular function of SMN and its role in the pathogenesis of SMA.

We gratefully acknowledge Dr. Marian DiFiglia for her help with synthetic SMN peptide design and antibody characterization and Jeremiah Scharf for his helpful comments on the manuscript. Digital scanning and printing of experimental data was done by Richard Milanich. The cDNA for human SMN was generously provided by Dr. Ching Wang and Dr. T. Conrad Gilliam of Columbia University. Mouse monoclonal anti-p80-coilin was a gift from Dr. Maria Carmo-Fonseca of the University of Lisbon, Portugal. Chicken anti-human SMN antisera C3 was provided by Dan Coovert and Dr. Arthur Burghes at Ohio State University. mAb 39.4D5, developed by T.M. Jessell, was obtained from the Developmental Studies Hybridoma Bank maintained by the Department of Pharmacology and Molecular Sciences, Johns Hopkins University School of Medicine, Baltimore, MD 21205, and the Department of Biological Sciences, University of Iowa, Iowa City, IA 52242, under contract N01-HD-2–3144 from the National Institute of Child Health and Human Development. R.H.B.'s laboratory receives support from the Amyotrophic Lateral Sclerosis Association, the Muscular Dystrophy Association, The C.B. Day Company, and National Institutes of Health Grants 5PO1Ag12992, 5RO1NS34913, and 5PO1NS31248. J.W.F. is supported by the American Paralysis Association and a National Research Service Award from the National Institutes of Health.

1. Crawford, T. O. & Pardo, C. A. (1996) *Neurobiol. Dis.* **3,** 97–110.
2. Brzustowicz, L. M., Lehner, T., Castilla, L. H., Penchaszadeh, G. K., Wilhelmsen, K. C., Daniels, R. J., Davies, K. E., Leppert, M., Ziter, F., Wood, D., *et al.* (1990) *Nature (London)* **344,** 540–541.
3. Gilliam, T. C., Brzustowicz, L. M., Castilla, L. H., Lehner, T., Penchaszadeh, G. K., Daniels, R. J., Byth, B. C., Knowles, J., Hislop, J. E., Saphira, Y., *et al.* (1990) *Nature (London)* **345,** 823–825.
4. Melki, J., Abdelhak, S., Sheth, P., Bachelot, M. F., Burlet, P., Marcadet, A., Aicardi, J., Barois, A., Carriere, J. P., Fardeau, M., *et al.* (1990) *Nature (London)* **344,** 767–768.
5. Lefebvre, S., Burglen, L., Reboullet, S., Clermont, O., Burlet, P., Viollet, L., Benichou, B., Cruaud, C., Millasseua, P., Zeviani, M., *et al.* (1995) *Cell* **80,** 155–165.
6. Lewin, B. (1995) *Cell* **80,** 1–5.
7. Brahe, C., Clermont, O., Zappata, S., Tiziano, F., Melki, J. & Neri, G. (1996) *Hum. Mol. Genet.* **5,** 1971–1976.
8. Bussaglia, E., Clermont, O., Tizzano, E., Lefebvre, S., Burglen, L., Cruaud, C., Urtizberea, J., Colomer, J., Munnich, A., Baiget, M. & Melki, J. (1995) *Nat. Genet.* **11,** 335–337.
9. Rodrigues, N. R., Owen, N., Talbot, K., Ignatius, J., Dubowitz, V. & Davies, K. E. (1995) *Hum. Mol. Genet.* **4,** 631–634.
10. Velasco, E., Valero, C., Valero, A., Moreno, F. & Hernandez-Chico, C. (1996) *Hum. Mol. Genet.* **5,** 257–263.
11. Hahnen, E., Schonling, J., Rudnik-Schoneborn, S., Raschke, H., Zerres, K. & Wirth, B. (1997) *Hum. Mol. Genet.* **6,** 821–825.
12. Parsons, D., McAndrew, P., Monani, U., Mendell, J., Burghes, A. & Prior, T. (1996) *Hum. Mol. Genet.* **5,** 1727–1732.
13. Talbot, K., Ponting, C. P., Theodosiou, A. M., Rodrigues, N. R., Surtees, R., Mountford, R. & Davies, K. E. (1997) *Hum. Mol. Genet.* **6,** 497–500.
14. Lefebvre, S., Burlet, P., Liu, Q., Bertrandy, S., Clermont, O., Munnich, A., Dreyfuss, G. & Melki, J. (1997) *Nat. Genet.* **16,** 265–269.
15. Coovert, D. C., Le, T. T., McAndrew, P. E., Strasswimmer, J., Crawford, T. O., Mendell, J. R., Coulson, S. E., Androphy, E. J., Prior, T. W. & Burghes, A. H. M. (1997) *Hum. Mol. Genet.* **6,** 1205–1214.
16. Liu, Q. & Dreyfuss, G. (1996) *EMBO J.* **15,** 3555–3565.
17. Liu, Q., Fischer, U., Wang, F. & Dreyfuss, G. (1997) *Cell* **90,** 1013–1021.
18. Fischer, U., Liu, Q. & Dreyfuss, G. (1997) *Cell* **90,** 1023–1029.
19. Battaglia, G., Principalle, A., Forti, F., Lizier, C. & Zeviani, M. (1997) *Hum. Mol. Genet.* **6,** 1961–1971.
20. Halpern, J. L., Habig, W. H., Neale, E. A. & Stibitz, S. (1990) *Infect. Immun.* **58,** 1004–1009.
21. Biedler, J. L., Helson, L. & Spengler, B. A. (1973) *Cancer Res.* **33,** 2643–2652.
22. Schreiber, E., Matthias, P., Muller, M. M. & Schaffner, W. (1989) *Nucleic Acids Res.* **17,** 6419.
23. Towbin, H., Staehelin, T. & Gordon, J. (1979) *Proc. Natl. Acad. Sci. USA* **76,** 4350–4354.
24. McCarthy, K. D. & de Vellis, J. (1980) *J. Cell Biol.* **85,** 890–902.
25. Tsuchida, T., Ensini, M., Morton, S. B., Baldassare, M., Edlund, T., Jessell, T. M. & Pfaff, S. L. (1994) *Cell* **79,** 957–970.
26. Chandler, C. S. & Ballard, F. J. (1986) *Biochem. J.* **237,** 123–130.
27. Schrank, B., Gotz, R., Gunnersen, J. M., Ure, J. M., Toyka, K. V., Smith, A. G. & Sendtner, M. (1997) *Proc. Natl. Acad. Sci. USA* **94,** 9920–9925.
28. Carmo-Fonseca, M., Ferreira, J. & Lamond, A. I. (1993) *J. Cell Biol.* **120,** 841–852.
29. Raska, I., Ochs, R. L., Andrade, L. E. C., Chan, E. K. L., Burlingame, R., Peebles, C., Gruol, D. & Tan, E. M. (1990) *J. Struct. Biol.* **104,** 120–127.
30. Gennarelli, M., Lucarelli, M., Capon, A., Merlini, L., Angelini, C., Novelli, G. & Dallapiccola, B. (1995) *Biochem. Biophys. Res. Commun.* **213,** 342–348.
31. Andrade, L. E. C., Tan, E. M. & Chan, E. K. L. (1993) *Proc. Natl. Acad. Sci. USA* **90,** 1947–1951.
32. Lamond, A. I. & Carmo-Fonseca, M. (1993) *Trends Cell Biol.* **3,** 198–204.